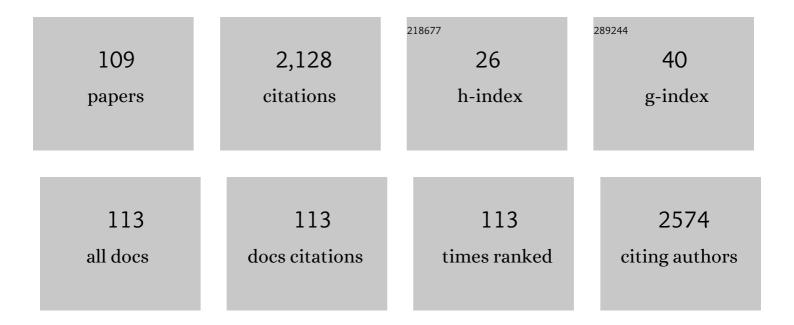
Ramon Escobar Galindo

List of Publications by Year in descending order

Source: https://exaly.com/author-pdf/2371992/publications.pdf Version: 2024-02-01



#	Article	IF	CITATIONS
1	Novel Mo–Si3N4 based selective coating for high temperature concentrating solar power applications. Solar Energy Materials and Solar Cells, 2014, 122, 217-225.	6.2	100
2	Oxidation tuning in AlCrN coatings. Surface and Coatings Technology, 2007, 201, 4505-4511.	4.8	95
3	Structure and properties of silver-containing a-C(H) films deposited by plasma immersion ion implantation. Surface and Coatings Technology, 2008, 202, 3675-3682.	4.8	87
4	Towards nanometric resolution in multilayer depth profiling: a comparative study of RBS, SIMS, XPS and GDOES. Analytical and Bioanalytical Chemistry, 2010, 396, 2725-2740.	3.7	79
5	Characterization of AISI 4140 borided steels. Applied Surface Science, 2010, 256, 2372-2379.	6.1	72
6	Structure–property relations in ZrCN coatings for tribological applications. Surface and Coatings Technology, 2010, 205, 2134-2141.	4.8	65
7	Growth of CrNx films by DC reactive magnetron sputtering at constant N2/Ar gas flow. Surface and Coatings Technology, 2006, 200, 6047-6053.	4.8	60
8	Ag ⁺ release inhibition from ZrCN–Ag coatings by surface agglomeration mechanism: structural characterization. Journal Physics D: Applied Physics, 2013, 46, 325303.	2.8	55
9	Diffusion model for growth of Fe ₂ B layer in pure iron. Surface Engineering, 2011, 27, 189-195.	2.2	52
10	Comparative depth-profiling analysis of nanometer-metal multilayers by ion-probing techniques. TrAC - Trends in Analytical Chemistry, 2009, 28, 494-505.	11.4	51
11	Influence of the oxygen partial pressure and post-deposition annealing on the structure and optical properties of ZnO films grown by dc magnetron sputtering at room temperature. Journal Physics D: Applied Physics, 2012, 45, 025303.	2.8	47
12	Influence of silver content on the tribomechanical behavior on Ag-TiCN bioactive coatings. Surface and Coatings Technology, 2012, 206, 2192-2198.	4.8	46
13	Ag–Ti(C, N)-based coatings for biomedical applications: influence of silver content on the structural properties. Journal Physics D: Applied Physics, 2011, 44, 375501.	2.8	42
14	Silver surface segregation in Ag-DLC nanocomposite coatings. Surface and Coatings Technology, 2015, 267, 90-97.	4.8	42
15	Silver activation on thin films of Ag–ZrCN coatings for antimicrobial activity. Materials Science and Engineering C, 2015, 55, 547-555.	7.3	38
16	Hybrid organic inorganic nylon-6/SiO2nanocomposites: Transport properties. Polymer Engineering and Science, 2004, 44, 1240-1246.	3.1	36
17	Influence of the nanoscale structural features on the properties and electronic structure of Al-doped ZnO thin films: An X-ray absorption study. Solar Energy Materials and Solar Cells, 2011, 95, 2341-2346.	6.2	35
18	<i>A Special Issue on</i> Advances in Solar Selective Nanostructures and Thin Films. Nanoscience and Nanotechnology Letters, 2013, 5, 1-2.	0.4	32

#	Article	IF	CITATIONS
19	Protrusion formation and surface porosity development on thermally annealed helium implanted copper. Nuclear Instruments & Methods in Physics Research B, 2004, 217, 262-275.	1.4	31
20	XRD and FTIR analysis of Ti–Si–C–ON coatings for biomedical applications. Surface and Coatings Technology, 2008, 203, 490-494.	4.8	31
21	First spectral emissivity study of a solar selective coating in the 150–600°C temperature range. Solar Energy Materials and Solar Cells, 2013, 117, 390-395.	6.2	31
22	Correlation between structure and optical properties in low emissivity coatings for solar thermal collectors. Thin Solid Films, 2010, 518, 5720-5723.	1.8	29
23	Improving the visible transmittance of low-e titanium nitride based coatings for solar thermal applications. Applied Surface Science, 2011, 258, 1784-1788.	6.1	28
24	Importance of the spectral emissivity measurements at working temperature to determine the efficiency of a solar selective coating. Solar Energy Materials and Solar Cells, 2015, 140, 249-252.	6.2	28
25	Design of high-temperature solar-selective coatings based on aluminium titanium oxynitrides AlyTi1â^'y(OxN1â^'x). Part 1: Advanced microstructural characterization and optical simulation. Solar Energy Materials and Solar Cells, 2018, 176, 81-92.	6.2	28
26	Bi-magnetic microwires: a novel family of materials with controlled magnetic behavior. Journal of Magnetism and Magnetic Materials, 2005, 290-291, 68-73.	2.3	27
27	Role of Y in the oxidation resistance of CrAlYN coatings. Applied Surface Science, 2015, 353, 504-511.	6.1	27
28	A modified blister test to study the adhesion of thin coatings based on local helium ion implantation. Thin Solid Films, 2005, 471, 170-176.	1.8	26
29	Interfacial effects during the analysis of multilayer metal coatings by radio-frequency glow discharge optical emission spectroscopy : Part 1. Crater shape and sputtering rate effects. Journal of Analytical Atomic Spectrometry, 2005, 20, 1108.	3.0	26
30	Improving the oxidation resistance of AlCrN coatings by tailoring chromium out-diffusion. Spectrochimica Acta, Part B: Atomic Spectroscopy, 2010, 65, 950-958.	2.9	26
31	A description of bubble growth and gas release during thermal annealing of helium implanted copper. Nuclear Instruments & Methods in Physics Research B, 2004, 217, 276-280.	1.4	24
32	Influence of spacer layer morphology on the exchange-bias properties of reactively sputtered <mml:math <br="" xmlns:mml="http://www.w3.org/1998/Math/MathML">display="inline"><mml:mrow><mml:mi mathvariant="normal">Co<mml:mo>a^•</mml:mo><mml:mi< td=""><td>3.2</td><td>24</td></mml:mi<></mml:mi </mml:mrow></mml:math>	3.2	24
33	mathvariant="normal">Agmultilayers. Physical Review B, 2007, 76, . Oxidation post-treatment of hard AlTiN coating for machining of hardened steels. Surface and Coatings Technology, 2009, 204, 256-262.	4.8	24
34	Long-term high temperature oxidation of CrAl(Y)N coatings in steam atmosphere. Corrosion Science, 2014, 80, 453-460.	6.6	24
35	Wear resistance of titanium–aluminium–chromium–nitride nanocomposite thin films. Vacuum, 2007, 81, 1453-1456.	3.5	23
36	Compositional and structural properties of nanostructured ZnO thin films grown by oblique angle reactive sputtering deposition: effect on the refractive index. Journal Physics D: Applied Physics, 2013, 46, 045306.	2.8	23

#	Article	IF	CITATIONS
37	Advanced surface characterization of silver nanocluster segregation in Ag–TiCN bioactive coatings by RBS, GDOES, and ARXPS. Analytical and Bioanalytical Chemistry, 2013, 405, 6259-6269.	3.7	22
38	Optical and electrical properties of the transparent conductor SrVO3 without long-range crystalline order. Applied Physics Letters, 2018, 112, .	3.3	22
39	Ag+ release and corrosion behavior of zirconium carbonitride coatings with silver nanoparticles for biomedical devices. Surface and Coatings Technology, 2013, 222, 104-111.	4.8	21
40	Design of high-temperature solar-selective coatings based on aluminium titanium oxynitrides AlyTi1-y(OxN1-x). Part 2: Experimental validation and durability tests at high temperature. Solar Energy Materials and Solar Cells, 2018, 185, 183-191.	6.2	20
41	Compositional depth profiling analysis of thin and ultrathin multilayer coatings by radio-frequency glow discharge optical emission spectroscopy. Surface and Coatings Technology, 2006, 200, 6185-6189.	4.8	19
42	Properties and Characterization of Hard Coatings Obtained by Boriding: An Overview. Defect and Diffusion Forum, 0, 297-301, 1284-1289.	0.4	19
43	Optical properties and refractive index sensitivity of reactive sputtered oxide coatings with embedded Au clusters. Journal of Applied Physics, 2014, 115, 063512.	2.5	19
44	Transparent conductive tantalum doped tin oxide as selectively solar-transmitting coating for high temperature solar thermal applications. Solar Energy Materials and Solar Cells, 2019, 196, 84-93.	6.2	19
45	Interfacial effects during the analysis of multilayer metal coatings by radio-frequency glow discharge optical emission spectroscopy : Part 2. Evaluation of depth resolution function and application to thin multilayer coatings. Journal of Analytical Atomic Spectrometry, 2005, 20, 1116.	3.0	17
46	An XPS and ellipsometry study of Cr–O–Al mixed oxides grown by reactive magnetron sputtering. Surface and Coatings Technology, 2011, 206, 1484-1489.	4.8	17
47	Nanometric resolution in glow discharge optical emission spectroscopy and Rutherford backscattering spectrometry depth profiling of metal (Cr, Al) nitride multilayers. Spectrochimica Acta, Part B: Atomic Spectroscopy, 2006, 61, 545-553.	2.9	15
48	Calibration of nitrogen content for GDOES depth profiling of complex nitride coatings. Journal of Analytical Atomic Spectrometry, 2007, 22, 1512.	3.0	15
49	Mechanisms of Oxidation of NdNiO _{3â^'δ} Thermochromic Thin Films Synthesized by a Two-Step Method in Soft Conditions. Journal of Physical Chemistry C, 2014, 118, 5908-5917.	3.1	15
50	Determination of the Optical Constants of Gold Nanoparticles from Thin-Film Spectra. Journal of Physical Chemistry C, 2015, 119, 9450-9459.	3.1	14
51	Advanced characterization and optical simulation for the design of solar selective coatings based on carbon: transition metal carbide nanocomposites. Solar Energy Materials and Solar Cells, 2016, 157, 580-590.	6.2	14
52	Surface characterization of Ti-Si-C-ON coatings for orthopedic devices: XPS and Raman spectroscopy. Solid State Sciences, 2011, 13, 95-100.	3.2	13
53	Coordination chemistry of titanium and zinc in Ti(1â^'x)Zn2xO2 (0 ≤≤1) ultrathin films grown by DC reactive magnetron sputtering. RSC Advances, 2012, 2, 2696.	3.6	13
54	Structural and mechanical properties of Au alloyed AlO sputter deposited coatings. Surface and Coatings Technology, 2012, 206, 2740-2745.	4.8	12

#	Article	IF	CITATIONS
55	Ag-N dual acceptor doped p-type ZnO thin films by DC reactive magnetron co-sputtering. Materials Letters, 2016, 181, 12-15.	2.6	12
56	Influence of the surface morphology and microstructure on the biological properties of Ti–Si–C–N–O coatings. Thin Solid Films, 2010, 518, 5694-5699.	1.8	11
57	Formation of antireflection Zn/ZnO core–shell nano-pyramidal arrays by O ₂ ⁺ ion bombardment of Zn surfaces. Nanoscale, 2017, 9, 14201-14207.	5.6	11
58	Influence of the yttria content on the mechanical properties of Y2O3-ZrO2 thin films prepared by EB-PVD. Vacuum, 2007, 81, 1457-1461.	3.5	10
59	Modelling of Glow Discharge Optical Emission Spectroscopy depth profiles of metal (Cr,Ti) multilayer coatings. Spectrochimica Acta, Part B: Atomic Spectroscopy, 2008, 63, 422-430.	2.9	10
60	Characterization of rough interfaces obtained by boriding. Applied Surface Science, 2008, 255, 2596-2602.	6.1	10
61	High- and low-energy x-ray photoelectron techniques for compositional depth profiles: destructive versus non-destructive methods. Journal Physics D: Applied Physics, 2013, 46, 065310.	2.8	10
62	Highâ€Rate Deposition of Stoichiometric Compounds by Reactive Magnetron Sputtering at Oblique Angles. Plasma Processes and Polymers, 2016, 13, 960-964.	3.0	10
63	Aperiodic Metalâ€Dielectric Multilayers as Highly Efficient Sunlight Reflectors. Advanced Optical Materials, 2017, 5, 1600833.	7.3	10
64	Positron beam analysis of structurally ordered porosity in mesoporous silica thin films. Materials Science and Engineering B: Solid-State Materials for Advanced Technology, 2003, 102, 2-7.	3.5	9
65	Effect of the Incorporation of Titanium on the Optical Properties of ZnO Thin Films: From Doping to Mixed Oxide Formation. Coatings, 2019, 9, 180.	2.6	9
66	Depth-selective 2D-ACAR studies on low-k dielectric thin films. Radiation Physics and Chemistry, 2003, 68, 357-362.	2.8	8
67	Stress reduction in a-C:H coatings through the addition of nitrogen to the feed gas. Diamond and Related Materials, 2004, 13, 1645-1657.	3.9	8
68	Structural and Mechanical properties of Ti–Si–C–ON for biomedical applications. Surface and Coatings Technology, 2008, 202, 2403-2407.	4.8	8
69	Influence of excesses of volatile elements on structure and composition of solution derived lead-free (Bi 0.50 Na 0.50) 1x Ba x TiO 3 thin films. Journal of the European Ceramic Society, 2016, 36, 89-100.	5.7	8
70	Structural effects due to the incorporation of Ar atoms in the lattice of ZrO2 thin films prepared by ion beam assisted deposition. Nuclear Instruments & Methods in Physics Research B, 2002, 194, 333-345.	1.4	7
71	Systematic positron study of hydrophilicity of the internal pore surface in ordered low-k silica thin films. Materials Science and Engineering B: Solid-State Materials for Advanced Technology, 2003, 102, 403-408.	3.5	7
72	Determination of Boron Diffusion Coefficients in Borided Tool Steels. Defect and Diffusion Forum, 2009, 283-286, 681-686.	0.4	7

#	Article	IF	CITATIONS
73	Molybdenum Interlayers for Nucleation Enhancement in Diamond CVD Growth. Journal of Nanoscience and Nanotechnology, 2010, 10, 2885-2891.	0.9	7
74	Control of the optical properties of silicon and chromium mixed oxides deposited by reactive magnetron sputtering. Thin Solid Films, 2011, 519, 3509-3515.	1.8	7
75	Morphotropic Phase Boundary in Solutionâ€Derived (<scp><scp>Bi</scp></scp> >ac/scp>/sub>) _{1â^'<i>x</i>Thin Films: Part I Crystalline Structure and Compositional Depth Profile. Journal of the American Ceramic Society. 2014. 97. 1269-1275.}	/sub> <scp></scp>	<scp>Ba</scp>
76	Electrochemical vs antibacterial characterization of ZrCN–Ag coatings. Surface and Coatings Technology, 2015, 275, 357-362.	4.8	7
77	Stoichiometric Control of SiO _x Thin Films Grown by Reactive Magnetron Sputtering at Oblique Angles. Plasma Processes and Polymers, 2016, 13, 1242-1248.	3.0	7
78	On the Effect of Thin Film Growth Mechanisms on the Specular Reflectance of Aluminium Thin Films Deposited via Filtered Cathodic Vacuum Arc. Coatings, 2018, 8, 321.	2.6	7
79	Study of polymer/metal coating under stress using positron annihilation spectroscopy. Acta Materialia, 2000, 48, 4743-4747.	7.9	6
80	Adhesion behaviour of CrNx coatings on pre-treated metal substrates studied in situ by PBA and ESEM after annealing. Surface and Coatings Technology, 2005, 199, 57-65.	4.8	6
81	Beneficial silver: antibacterial nanocomposite Ag-DLC coating to reduce osteolysis of orthopaedic implants. Journal of Physics: Conference Series, 2010, 252, 012005.	0.4	6
82	In-depth multi-technique characterization of chromium–silicon mixed oxides produced by reactive ion beam mixing of the Cr/Si interface. Journal of Analytical Atomic Spectrometry, 2012, 27, 390.	3.0	6
83	Comparative Study of Micro- and Nano-structured Coatings for High-Temperature Oxidation in Steam Atmospheres. Oxidation of Metals, 2014, 81, 227-236.	2.1	6
84	Dynamics of GDOES-induced surface roughening in metal interfaces. Analytical and Bioanalytical Chemistry, 2014, 406, 7483-7495.	3.7	6
85	High-temperature solar-selective coatings based on Cr(Al)N. Part 2: Design, spectral properties and thermal stability of multilayer stacks. Solar Energy Materials and Solar Cells, 2020, 218, 110812.	6.2	6
86	Positronium formation in NaY-zeolites studied by lifetime, positron beam Doppler broadening and 3-gamma detection techniques. Radiation Physics and Chemistry, 2000, 58, 715-718.	2.8	5
87	In situ mechanical, temperature and gas exposure treatments of materials combined with variable energy positron beam techniques. Applied Surface Science, 2002, 194, 239-244.	6.1	5
88	Optical and transport properties of Tiâ€doped In ₂ O ₃ thin films prepared by electron beam physical vapour deposition. Physica Status Solidi (A) Applications and Materials Science, 2010, 207, 1549-1553.	1.8	5
89	Structural and optical characterization of nanostructured ZnO grown on alumina templates. Materials Research Express, 2014, 1, 045028.	1.6	5
90	Cluster Tool for In Situ Processing and Comprehensive Characterization of Thin Films at High Temperatures. Analytical Chemistry, 2018, 90, 7837-7842.	6.5	5

91 Synthess and Characterisation of ASA-PEEK Composites for Fused Filament Fabrication. Polymers. 4.5 4.6 92 Biccompatible Silver containing a CH and a C coatings: A Comparative Study. Materials Research 0.1 8 93 Accult 2 club 0 or aph 3 club 2 clob aph 2 club and a C coatings: A Comparative Study. Materials Research 0.1 8 94 Materials Research 2.8 3 95 Fabrication of the optiodecronic properties and corrosion behavior of Applications Using Non-Blased 2.6 3 96 Saloring Crystalline Structure of Titanium Oxide Films for Optical Applications Using Non-Blased 2.6 3 97 The design of an electrostatic variable energy position beam for studies of defects in ceramic 0.1 2 98 Veerged thin thins analyzed by Clow Discharge Optical Emission Spectroscopy. Thin Sold Films, 2008, 516, 1.8 2 99 Influence of the Rentro Layer composition in the metalist properties of solar selective coatings. 1.8 2 90 Research and anyced by Clow Discharge Optical Emission Spectroscopy. Thin Sold Films, 2008, 516, 1.8 2 2 91 Influence of the Rentro Layer composition in the metalist properties of solar selective coatings. 1.8 1 92 Influence of the Rentro Layer compo	#	Article	IF	CITATIONS
92 Sockety Symposia Proceedings, 2006, 950, 1. 0.1 3 93 Lealuation of the optoelectronic properties and concision behavior of Alegaby Sciebb Organ Sciebb-Organ Can Offmis prepared by dc pulsed magnetron sputtering, Journal Physics D: Applied Physics, 2014, 47, 485501. 2.8 3 94 Influence of culture media on the physical and chemical properties of Ag&CTICN coatings, Journal Physics D: Applied Physics, 2014, 47, 335401. 2.8 3 95 Tailoring Crystalline Structure of Tianium Oxide Films for Optical Applications Using Non-Blased Physics Cathodic Vacuum Arc Deposition at Room Temperature. Coatings, 2021, 11, 233. 2.6 3 96 Solar selective coatings and materials for high-temperature solar thermal applications. J. 2021, 1 3 97 The design of an electrostatic variable energy positron beam for studies of defects in ceramic coatings and polymer films. Applied Surface Science, 2002, 194, 4751. 6.1 2 98 Wder Pd thin films analyzed by Clow Discharge Optical Emission Spectroscopy. Thin Solid Films, 2008, 516, 524-6530. 1.8 2 99 Influence of the Remirco law endoced trains, 2014, 577, 316-520. 1.8 2 90 Nano-porosity in solid animation of anorphous hydrogenated carbon coatings monitored by positron ambitation. This Solid Films, 2003, 63, 1133-1139. 7.8 1 100 Nano-porosity in solid films, 2005, 47/8, 338-34	91		4.5	4
93 Alrcubs 24 (subs 24 (subs 24 (subs)-doied 22n0 films prepared by dc pulsed magnetron sputtering, Journal Physics 2014, 47, 45501. 2.8 3 94 Influence of culture media on the physical and chemical properties of Ag36"TICN coatings, Journal Physics, 2014, 47, 335401. 2.8 3 95 Tailoring Crystalline Structure of Ttanhum Oxide Films for Optical Applications Using Non-Blased Physics, 2014, 47, 335401. 3 96 Solar selective coatings and materials for high-temperature. Coatings, 2021, 11, 233. 3 97 The design of an electrostatic worlable energy positron beam for studies of defects in ceramic coatings and polymer films. Applied Surface Science, 2002, 194, 4751. 6.1 2 98 Hydrogen and oxygen in-depth evolution during electrochemical hydrogenation/dehydrogenation of Yae PR thin films analyzed by Clow Discharge Optical Emission Spectroscopy. Thin Solid Films, 2006, 516, 5524 6530. 1.8 2 99 Influence of the IR mirror layer composition in the mechanical properties of solar selective coatings in the mechanical properties of solar selective coatings 1.8 2 100 Nano-porosity in silica reinforced methyltrimethoxylane coatings studied by positron beam analysis. 7.8 1 101 Thermally induced delamination of amorphous hydrogenated carbon coatings monitored by positron in the amalysis. Surface and Coatings Technology, 2004, 180-181, 207-212. 1.9 1	92		0.1	3
94 Physics D: Applied Physics, 2014, 47, 335401. 2.3 3 95 Tailoring Crystalline Structure of Titanium Oxide Films for Optical Applications Using Non-Blased 2.0 3 96 Solar selective coatings and materials for high-temperature. Coatings, 2021, 11, 233. 2.0 3 97 The design of an electrostatic variable energy positron beam for studies of defects in ceramic coatings and polymer films. Applied Surface Science, 2002, 194, 47-51. 6.1 2 98 Yéfer Pithin films analyzed by Clow Discharge Optical Emission Spectroscopy. Thin Solid Films, 2008, 516, 524-6530. 1.8 2 99 Influence of the IR mitror layer composition in the mechanical properties of solar selective coatings made from MocSISN4 cermet. Thin Solid Films, 2014, 571, 316-520. 1.8 2 100 Nano-porosity in silica reinforced methyltrimethoxysilane coatings studied by positron beam analysis. Composites Science and Technology, 2003, 63, 1133-1139. 7.8 1 101 Thermally induced delamination of amorphous hydrogenated carbon coatings monitored by positron 4.8 1 102 Interface detection in poly-ethylene terephthalatea@"metal laminates using variable energy positron 1.8 1 101 Interface detection in poly-ethylene terephthalatea@"metal laminates using variable energy positron 1.8 1 <td< td=""><td>93</td><td>Al₂O₃-doped ZnO films prepared by dc pulsed magnetron sputtering. Journal</td><td>2.8</td><td>3</td></td<>	93	Al ₂ O ₃ -doped ZnO films prepared by dc pulsed magnetron sputtering. Journal	2.8	3
90 Filtered Cathodic Vacuum Arc Deposition at Room Temperature. Coatings, 2021, 11, 233. 240 3 96 Solar selective coatings and materials for high-temperature solar thermal applications., 2021, , 383.427. 3 97 The design of an electrostatic variable energy positron beam for studies of defects in ceramic coatings and polymer films. Applied Surface Science, 2002, 194, 47-51. 6.1 2 98 Hydrogen and oxygen in-depth evolution during electrochemical hydrogenation/dehydrogenation of Y4E*Pd thin films analyzed by Clow Discharge Optical Emission Spectroscopy. Thin Solid Films, 2008, 516, 652445530. 1.8 2 99 Influence of the IR-mirror layer composition in the mechanical properties of solar selective coatings made from MotSi3N4 cermet. Thin Solid Films, 2014, 571, 316-320. 1.8 2 100 Nano-porosity in silica reinforced methyltrimethoxysilane coatings studied by positron beam analysis. Composites Science and Technology, 2003, 63, 1133-1139. 7.8 1 101 Thermally induced delamination of amorphous hydrogenated carbon coatings monitored by positron beam analysis. Surface and Coatings Technology, 2004, 180-181, 207-212. 4.8 1 102 Interface detection in poly-ethylene terephthalateae* metal laminates using variable energy positron annihilation. Thin Solid Films, 2005, 478, 338-344. 1 103 Comprehensive Environmental Testing of Optical Properties in Thin Films. Proceedia CIRP, 2014, 22, 271-276.	94		2.8	3
383 427. 3 97 The design of an electrostatic variable energy positron beam for studies of defects in ceramic coatings and polymer films. Applied Surface Science, 2002, 194, 47-51. 6.1 2 98 Hydrogen and oxygen in-depth evolution during electrochemical hydrogenation/dehydrogenation of Y46°Pd thin films analyzed by Clow Discharge Optical Emission Spectroscopy. Thin Solid Films, 2008, 516, 524-6530. 1.8 2 99 Influence of the IR-mirror layer composition in the mechanical properties of solar selective coatings made from MoSIBN4 cermet. Thin Solid Films, 2014, 571, 316-320. 1.8 2 100 Nano-porosity in silica reinforced methyltrimethoxysilane coatings studied by positron beam analysis. Composites Science and Technology, 2003, 63, 1133-1139. 7.8 1 101 Thermally induced delamination of amorphous hydrogenated carbon coatings monitored by positron beam analysis. Surface and Coatings Technology, 2004, 180-181, 207-212. 4.8 1 102 Interface detection in poly-ethylene terephthalateãe" metal laminates using variable energy positron annihilation. Thin Solid Films, 2005, 478, 338-344. 1.8 1 103 Comprehensive Environmental Testing of Optical Properties in Thin Films. Procedia CIRP, 2014, 22, 1.9 1 1 104 (Bilkitsub>t) Skit/sub>t) Skit/sub>t) Skit/sub>t) Skit/sub>t) Skit/sub>t, Skit/sub>t, Skit/sub>t, Skit/sub>t, Skit/sub>t, Skit/sub>t, Skit/sub>t, Skit/sub>t, Skit/sub>t	95		2.6	3
97 coatings and polymer films. Applied Surface Science, 2002, 194, 47-51. 0-1 2 98 Hydrogen and oxygen in-depth evolution during electrochemical hydrogenation/dehydrogenation of YAE"Pd thin films analyzed by Clow Discharge Optical Emission Spectroscopy. Thin Solid Films, 2008, 516, 524-6530. 1.8 2 99 Influence of the IR-mirror layer composition in the mechanical properties of solar selective coatings made from Mox5i3N4 cermet. Thin Solid Films, 2014, 571, 316-320. 1.8 2 100 Nano-porosity in silica reinforced methyltrimethoxysilane coatings studied by positron beam analysis. Composites Science and Technology, 2003, 63, 1133-1139. 7.8 1 101 Thermally induced delamination of amorphous hydrogenated carbon coatings monitored by positron beam analysis. Surface and Coatings Technology, 2004, 180-181, 207-212. 4.8 1 102 Interface detection in poly-ethylene terephthalateãe"metal laminates using variable energy positron annihilation. Thin Solid Films, 2005, 478, 338-344. 1 103 Comprehensive Environmental Testing of Optical Properties in Thin Films. Procedia CIRP, 2014, 22, 1.9 1 104 the Arystality, sub> 0.5</, sub> 0.5</, sub> 0.5</, sub> 1.x</, sub> Ba< sub> TiQ</, sub> 3</, s	96			3
98 Yå@"Pd thin films änalyzed by Glow Discharge Öptical Emission Spectroscopy. Thin Solid Films, 2008, 516, 6524-6530. 1.8 2 99 Influence of the IR-mirror layer composition in the mechanical properties of solar selective coatings made from MoSi3N4 cernet. Thin Solid Films, 2014, 571, 316-320. 1.8 2 100 Nano-porosity in silica reinforced methyltrimethoxysilane coatings studied by positron beam analysis. Composites Science and Technology, 2003, 63, 1133-1139. 7.8 1 101 Thermally induced delamination of amorphous hydrogenated carbon coatings monitored by positron beam analysis. Surface and Coatings Technology, 2004, 180-181, 207-212. 4.8 1 102 Interface detection in poly-ethylene terephthalateà6("metal laminates using variable energy positron annihilation. Thin Solid Films, 2005, 478, 338-344. 1.8 1 103 Comprehensive Environmental Testing of Optical Properties in Thin Films. Procedia CIRP, 2014, 22, 1.9 1 104 the crystalline structure in (Bi&Ritsub> 0.5&Rit/sub> 0.5&Rit/sub> 1.4&Rit/sub>	97	The design of an electrostatic variable energy positron beam for studies of defects in ceramic coatings and polymer films. Applied Surface Science, 2002, 194, 47-51.	6.1	2
99 made from MotSi3N4 cermet. Thin Solid Films, 2014, 571, 316-320. 1-8 2 100 Nano-porosity in silica reinforced methyltrimethoxysilane coatings studied by positron beam analysis. Composites Science and Technology, 2003, 63, 1133-1139. 7.8 1 101 Thermally induced delamination of amorphous hydrogenated carbon coatings monitored by positron beam analysis. Surface and Coatings Technology, 2004, 180-181, 207-212. 4.8 1 102 Interface detection in poly-ethylene terephthalateâ€"metal laminates using variable energy positron annihilation. Thin Solid Films, 2005, 478, 338-344. 1.8 1 103 Comprehensive Environmental Testing of Optical Properties in Thin Films. Procedia CIRP, 2014, 22, 271-276. 1.9 1 104 Evolution of the crystalline structure in (Bi _{0.5} 0.50.50.51.x1.x33333333333333333333333333333333333333333333333333333333333&	98	Yấ€"Pḋ thin films analyzed by Clow Discharge Öptical Emission Spectroscopy. Thin Solid Films, 2008, 516,	1.8	2
100 Composites Science and Technology, 2003, 63, 1133-1139. 7.8 1 101 Thermally induced delamination of amorphous hydrogenated carbon coatings monitored by positron beam analysis. Surface and Coatings Technology, 2004, 180-181, 207-212. 4.8 1 102 Interface detection in poly-ethylene terephthalate–metal laminates using variable energy positron annihilation. Thin Solid Films, 2005, 478, 338-344. 1.8 1 103 Comprehensive Environmental Testing of Optical Properties in Thin Films. Procedia CIRP, 2014, 22, 271-276. 1.9 1 104 Evolution of the crystalline structure in (Bi _{0.5} 0.50.51.xBa _{TiQ₃3} 3333333333333333333333333333333333333333333333333333333333333333333333333333	99	Influence of the IR-mirror layer composition in the mechanical properties of solar selective coatings made from Mo:Si3N4 cermet. Thin Solid Films, 2014, 571, 316-320.	1.8	2
101 beam analysis. Surface and Coatings Technology, 2004, 180-181, 207-212. 4.3 1 102 Interface detection in poly-ethylene terephthalate–metal laminates using variable energy positron annihilation. Thin Solid Films, 2005, 478, 338-344. 1.8 1 103 Comprehensive Environmental Testing of Optical Properties in Thin Films. Procedia CIRP, 2014, 22, 271-276. 1.9 1 104 Evolution of the crystalline structure in (Bi _{0.5} 0.50.51-xBa _X TiQ ₃ 3 _{3₃3₃3} 33333333333333333333333333333333333333333333333333333333333333333333333333333333333333333 <td>100</td> <td></td> <td>7.8</td> <td>1</td>	100		7.8	1
102 annihilation. Thin Solid Films, 2005, 478, 338-344. 1.8 1.8 1 103 Comprehensive Environmental Testing of Optical Properties in Thin Films. Procedia CIRP, 2014, 22, 271-276. 1.9 1 104 Evolution of the crystalline structure in (Bi _{0.5}) _{1-x} Ba _x TiO ₃ 3333333333333333333333333333333333333333333333333333333333333333333333333333333333333333333333333333333333333333333 </td <td>101</td> <td>Thermally induced delamination of amorphous hydrogenated carbon coatings monitored by positron beam analysis. Surface and Coatings Technology, 2004, 180-181, 207-212.</td> <td>4.8</td> <td>1</td>	101	Thermally induced delamination of amorphous hydrogenated carbon coatings monitored by positron beam analysis. Surface and Coatings Technology, 2004, 180-181, 207-212.	4.8	1
103 271-276. 1.9 1 Evolution of the crystalline structure in (Bi _{0.5} Na _{0.5}) _{1-x} Ba _X TiO _{3coatingsâ€â€™ by V. Hoffmann, J. Anal. At. Spectrom., 2008, 23, DOI: 10.1039/b713743p. Journal of Analytical 3.0 0 Impact of the particles impingement on the electronic conductivity of Al doped ZnO films grown by reactive magnetron sputtering. IOP Conference Series: Materials Science and Engineering, 2010, 12, 0.6 0.6 0}	102	Interface detection in poly-ethylene terephthalate–metal laminates using variable energy positron annihilation. Thin Solid Films, 2005, 478, 338-344.	1.8	1
 (Bi<sub>0.5</sub>Na<sub>0.5</sub>)<sub>1-x</sub>Ba<sub>Xa</sub>TiQ<sub>3</sub>3</sub>3</sub>3</sub>3</sub>3</sub>3</sub>3</sub>3</sub>3</sub>3</sub>3</sub>3</sub>3</sub>3</sub>3</sub>3</sub>3</sub>3</sub>3</sub>3</sub>3</sub>3</sub>3</sub>3</sub>3</sub>3</sub>3</sub>3</sub>3</sub>3</sub>3</sub>3</sub>3</sub>3</sub>3</sub>3</sub>3</sub>3</sub>3</sub>3</sub>3</sub>3</sub>3</sub>3</sub>3</sub>3</sub>3</sub>3</sub>3</sub>3</sub>3</sub>3</sub>3</sub>3</sub>3</sub>3</sub>3</sub>3</sub>3</sub>3</sub>3</sub>3</sub>3</sub>3</sub>3</sub>3</sub>3</sub>3</sub>3</sub>3</sub>3</sub>3</sub>3</sub>3</sub>3</sub>3</sub>3</sub>3</sub>3</sub>3</sub>3</sub>3</sub>3</sub>3</sub>3</sub>3</sub>3</sub>3</sub>3</sub>3</sub>3</sub>3</sub>3</sub>3</sub>3</sub>3</sub>3</sub>3</sub>3</sub>3</sub>3</sub>3</sub>3</sub>3</sub>3</sub>3</sub>3</sub>3</sub>3</sub>3</sub>3</sub>3</sub>3</sub>3</sub>3</sub>3</sub>3</sub>3</sub>3</sub>3</sub>3</sub>3</sub>3</sub>3</sub>3</sub>3</sub>3</sub>3</sub>3</sub>3</sub>3</sub>3</sub>3</sub>3</sub>3</sub>3</sub>3</sub>3</sub>3</sub>3</sub>3</sub>3</sub>3</sub>3</sub>3</sub>3</sub	103		1.9	1
 coatingsâ€â€™ by V. Hoffmann, J. Anal. At. Spectrom., 2008, 23, DOI: 10.1039/b713743p. Journal of Analytical 3.0 0 Atomic Spectrometry, 2008, 23, 593. Impact of the particles impingement on the electronic conductivity of Al doped ZnO films grown by reactive magnetron sputtering. IOP Conference Series: Materials Science and Engineering, 2010, 12, 0.6 0 012006. 	104	(Bi _{0.5} Na _{0.5}) _{1-x} Ba _{xthin films around the Morphotropic Phase Boundary. Boletin De La Sociedad Espanola De Ceramica Y}	;TiO <su 1.9</su 	b>3
106 reactive magnetron sputtering. IOP Conference Series: Materials Science and Engineering, 2010, 12, 0.6 0 012006. 0 0 0 0	105	coatingsâ€â€™ by V. Hoffmann, J. Anal. At. Spectrom., 2008, 23, DOI: 10.1039/b713743p. Journal of Analytical	3.0	0
Room temperature deposition of highly dense TiO2thin films by filtered cathodic vacuum arc. , 2015, , . 0	106	reactive magnetron sputtering. IOP Conference Series: Materials Science and Engineering, 2010, 12,	0.6	0
	107	Room temperature deposition of highly dense TiO2thin films by filtered cathodic vacuum arc. , 2015, , .		0

108 Solar selective coatings based on carbon: transition metal nanocomposites. , 2015, , .

0

#	Article	IF	CITATIONS
109	Comprehensive microstructural and optical characterization of the thermal stability of aluminum-titanium oxynitride thin films after high temperature annealing in air. Emergent Materials, 2021, 4, 1559-1568.	5.7	0